Stockholm
University

June 16, 2010

MASTER DEGREE PROJECT IN METEOROLOGY
30 ECTS CREDITS

Evaluation of calculated concentrations of air pollution in the Stockholm region – comparison with measurements

Author	**Supervisor**
Adam Dingwell	Christer Johansson
addi9884@student.su.se	christer@slb.nu
Assistant Supervisor	**Contact Supervisor**
Magnuz Engardt	Jörg Gumbel
magnuz.engardt@smhi.se	gumbel@misu.su.se

Abstract

The aim of this project was to evaluate atmospheric dispersion models. Two model were used; An Eulerian transport model model, MATCH (Multi-scale Atmospheric Transport and CHemistry), and a Gaussian plume model, both developed by SMHI (Swedish Meteorological and Hydrological Institute). As the name suggests, MATCH can be applied over different scales, *e.g.* Europe, Sweden or smaller region such as Stockholm-Uppsala county. In this project the MATCH model was first run covering Europe, then run locally covering Stockholm and Uppsala with a finer resolution, using the result from the European run as boundary values. The Gaussian model is designed specifically for modelling urban pollution. It calculates the pollution concentrations directly from Gaussian plume equations based on the current or future weather conditions. The models were tested for several winter periods and compared to each other for February 2010. The performance was evaluated by comparing the model results with observations at specific points within the model domains. The main trace species were Nitrogen Oxides, NO_x, and Particulate Matter, PM_{10}.

The Gauss model performed better than the MATCH model when comparing calculated NO_x-concentrations with urban observations. MATCH results were closer to observations at the rural site than the urban. This suggests that the resolution (2×2 km) used in the MATCH runs was too rough to simulate the strong variation in pollutants in an urban environment. Different temporal resolutions of boundary values (*i.e.* data at the edge of the model domain) for the MATCH model was tested. This showed that reading boundary values once per 24 hours is insufficient, and that the higher resolution of new boundary values every 6 hours is adviced. Attempts to simulate PM_{10} using the Gauss model failed since the observed concentrations were completely dominated by long distance transport during the entire month. This turned out to be due to persistent road wetness, preventing suspension of particles from road sources.

Contents

1 introduction

The aim of this project was to evaluate the performance of atmospheric dispersion models in the Stockholm region as well as to identify the reasons behind possible deviations from observations.

With the increasing knowledge about the negative health effects from air pollution, a growing demand of reliable methods to measure or otherwise estimate air quality follows. While observations are often accepted as a good representation of reality, they only show the values at the observation site. Therefore, models provide an important complement where observations are unavailable. Developing reliable dispersion models allows us to make predictions of air quality and it allows us to study the effects of different scenarios when expanding infrastructure, or planning ahead when building new residental areas to optimize environmental conditions.

Evaluation of model performance is made by comparing the model results with observations. The idea is that if the model results coincide with measurements at observation sites located within the model domain, the model should describe the pollution correctly, even when and where observations are unavailable.

2 Theory

An air pollutant is a substance in the air which is known to cause health problems or damage to the environment. The pollutants can be gases or suspended liquid droplets or solid particles. Sources can be either natural on anthropogenic. This study focuses on NO_x, (*i.e.* nitric oxide, NO, and nitrogen dioxide, NO_2, together) and particulate matter of typical diameters less than 10 μm (PM_{10}).

NO_x is used rather than NO or NO_2 since these are very reactive species, while the general NO_x content is more stable. NO_x is primarily emitted into the atmosphere in the form of NO, which during daytime rapidly establishes an steady state with NO_2 by the following null cycle, (Wallace and Hobbs , 2006):

$$NO + O_3 \rightarrow NO_2 + O_2 \qquad (1)$$
$$NO_2 + O_2 + M + h\nu \rightarrow NO + O_3 + M \quad (2)$$
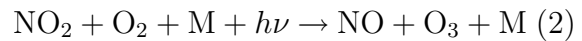
where M is an inert molecule absorbing excess molecular energy and $h\nu$.

Particulate matter is either liquid droplets or solid particles (or a combination of the two) suspended in the atmosphere. The main anthropogenic sources of PM are dust from roads, wind erosion of tilled land, biomas bruning, fuel combustion and industrial processes (Wallace and Hobbs , 2006). Particulates can either be primary, *i.e.* emitted as particles, or secondary, *i.e.* formed in the atmosphere through condensation of gases, (*i.e.* g-to-p conversion).

Two models were studied in this project, an Eulerian grid model, MATCH (Multi-scale Atmospheric Transport and CHemistry), and a Gaussian model. A grid model uses numerical solutions to the equations of motion over a domain divided into numerous interacting grid boxes. A Gaussian model uses Gaussian plume theory to form completely analytical equations describing the dispersion from a single or numerous sources. The calculations can in both cases be driven by either observed or predicted meteorology. The main trace species studied was nitrogen oxides (NO_x) and particulate matter (PM_{10}), other species treated by MATCH include ozone, sulphur-dioxide, sulphate and volatile organic compounds (VOC).

2.1 Measurements

Measurements are made for NO_x and particulate matter of sizes $< 10\mu m$ (PM_{10}). Particulate Matter (PM), is measured by leading the air sample through a vibrating filter, perpendicular to the vibration plane. Due to intertia, the vibration frequency of the grid is dependent on the mass of the particulates passing through it. Thus by measuring the frequency it is possible to calculate the PM-mass.

NO_x is measured using the chemiluminescence method.This method uses the fast reaction between NO and O_3. The air sample is saturated with O_3, resulting in all NO being oxidized to NO_2 according to (1), some NO_2 molecules will be formed in excited state but will quickly degenerate to their ground state by emitting photons. The light intensity can be measured with high precision, and is converted to a voltage signal direclty proportional to the initial amount of NO.

In order to measure the total NO_x content ($NO+NO_2$), we also need to take into account the original NO_2 content. This is done by leading the air through a heated Molybdenum converter, which reduces the NO_2 to NO, before measuring NO. Instruments measuring NO_x are very sensitive and needs to be regularly calibrated, the instruments used are automatcally calibrated once a day.

2.2 MATCH model

The MATCH model is a three dimensional Eulerian transport model developed by the Swedish Meteorological and Hydrological Institute (SMHI). It includes modules describing emissions, turbulent mixing, deposition, advection and chemistry. Required input includes emissions, meteorology, physiography and boundary concentration of trace species.

Meteorology is taken from a three dimensional numerical weather prediction model at regular intervals, normally once every six hours. This data is interpolated to give hourly values. Trace species are represented by mass mixing ratios. The boundary mixing ratios are based on observations at regional background locations or on previous larger scale model runs. The boundary values are read at regular intervals and interpolated in the same way as the meteorological data.

The advection scheme used in MATCH is Bott-type (Bott , 1999) with a fifth order scheme in the horizontal and a first or zeroth order in the vertical. For a complete description of the MATCH model, see Robertson et al. (1999).

MATCH is applicable for large scales, *e.g.* Europe, Sweden, single provinces. Since the model is Eulerian it should be able to simulate build up of trace species over longer time periods, as can be the case during long lasting inversion over urban areas. Modules describing different chemical schemes allows for easy adding or removing of different traces species from calculations.

2.3 Gauss model

The Airviro Gauss model is an analytical model which uses Gaussian plume theory.

Most Gaussian dispersion models run with a homogeneous wind field, the Airviro Gauss model however, can run with realistic wind profiles. These profiles are calculated using a method described by Danard (1976). The method is based on the assumption that the surface wind can be estimated from mesoscale influences of orography, friction and heating together with the large scale wind in the free atmosphere (the free wind). The free wind is calculated from observations at a 50 m mast in Högdalen (suburban area south of Stockholm), using methods described by Holt-

slag (1984).

The model is based on the Gaussian plume equation, which can be found in books on dispersion modelling, *e.g.* Zannetti (1990):

$$C = \frac{Q}{2\pi\sigma_y\sigma_z U}\, e^{\frac{-y^2}{2\sigma_y^2}} \cdot X \qquad (3)$$

where Q is the emission rate, U is the horizontal wind velocity along the plume centerline, y is the crosswind distance from the plume centerline, σ_y and σ_z are the horizontal and vertical standard deviations of the emission distribution, respectively, and:

$$X = e^{\frac{-(z-h_e)^2}{2\sigma_z^2}} + e^{\frac{-(z+h_e)^2}{2\sigma_z^2}} + e^{\frac{-(z+h_e-2h)^2}{2\sigma_z^2}}$$

where z is the height above ground level and h_e is the plume height. The first term represents boundless vertical dispersion, the second and third terms represent the reflection at the ground and the top of the mixed layer, respectively.

The Gauss model solves Equation 3 along trajectories from the wind model. Furthermore, methods for estimating plume rise and building downwash are included. A more detailed description of the Gauss model is included in the *Airviro User's Reference*.

Since the model is analytical it is *very* computation efficient, however, since it does not "remember" previous pollution content, it is unable to simulate a long term build up. Another trade off is its inability to simulate transportation on larger scales. Therefore, rural observations are always required to consider long distant source distributions. However, it is useful when comparing the air quality of different areas within the city, and for studying different scenarios for infrastructure and building plans, since it is designed to work on urban scales.

2.4 Emissions

In both models, emissions are treated as coming from a point (*e.g.* chimney stacks), line (roads) or area (*e.g.* industrial areas, gas stations) or from an EDB. Where line and area sources are simulated by distributing point sources evenly along a line or over an area, respectively. The EDB collects the emissions from the line and area sources and creates a new ground level emission grid.

2.5 Statistical measures

In order to evaluate each model, the results were compared with observations using the statistical measures Fractional Bias (FB), Geometric Mean bias (MG), Normalized Mean Square Error (NMSE), Geometric Variance (VG), correlation (R) and the fraction of data within a factor of two from observations (FAC2) (as proposed by Chang and Hanna (2004)):

$$\mathrm{FB} = \frac{\overline{C_o} - \overline{C_p}}{0.5(\overline{C_o} + \overline{C_p})} \qquad (4)$$

$$\mathrm{MG} = \exp\left(\overline{\ln C_o} - \overline{\ln C_p}\right) \qquad (5)$$

$$\mathrm{NMSE} = \frac{\overline{(C_o - C_p)^2}}{\overline{C_o C_p}} \qquad (6)$$

$$\mathrm{VG} = \exp\left(\overline{(\ln C_o - \ln C_p)^2}\right) \qquad (7)$$

$$\mathrm{R} = \frac{\overline{(C_o - \overline{C_o})(C_p - \overline{C_p})}}{\sigma_{C_p}\sigma_{C_o}} \qquad (8)$$

$$\mathrm{FAC2} = \begin{array}{c}\text{fraction of data within:}\\ 0.5 \leq \frac{C_p}{C_o} \leq 2.0\end{array} \qquad (9)$$

where C_o represents observations, C_p the model predictions and σ_c is the standard deviation of the dataset.

FB measures the mean relative bias and indicates the linear systematic error. A positive FB indicates an under estimation by the model. MG also measures the mean relative bias, but is based on a logaritmic scale and represents the ratio of C_p

to C_o. NMSE and VG represent the linear and logarithmic mean relative scatter respectively, *i.e.* they cover both systematic and random errors. The linear measures may be overly influenced if the data contains several extreme outliers, in which case the logarithmic measures may provide a more balanced estimate. The logarithmic measures are more sensitive to extremely low values and undefined for zero values. R represents the linear relationship between observation and model, however, if there is strong non-linear relation it will not be represented by R. Furthermore R is very sensitive in the presence of few extreme outliers. FAC2 is applicable in most cases since it is not sensitive to the distribution of the variables or overly influenced by extreme outliers.

3 Measurement stations

The observations used in this study were made at two sites; a rooftop station at Torkel Knutssongatan (TK), away from any exceptional emission sources, and the remotely located Norr Malma (NM) outside Norrtälje. TK was used as the urban background station and NM as the rural station. In the main comparision we used the ARTEMIS (Assessment and Reliability of Transport Emission Models and Inventory Systems) emission model, which is an EU project ment to replace the numerous systems previously used by member states and create a standard emission model. It estimates the emissions based on the traffic load, road type, speed limits and the distribution of heavy/light traffic and fuel types.

4 MATCH settings

MATCH was run twice for each period. First using a low resolution grid (44 ×

44 km) covering Europe, yielding the boundry values for the second run. The second (local) run was made covering Uppsala and Stockholm counties, with a finer resolution (2 × 2 km) . Meteorology was taken from HIRLAM. Two periods where used, January and February 2010, separately. January was initially run with three different settings to check the influence of plume rise. The first run had no plume rise and emitted everything in the lowermost level (0-60 m), the second and third run added a plume rise of 50% of the chimney height. The first two runs were driven by meteorology from a (22 × 22 km) grid, the third run used meteorology from a (11 × 11 km) grid.

Due to a lack of data from the rural observation site at Norr Malma, preventing a complete evaluation, MATCH was run over February as well. This period, however, lacked boundry values at the same resolution in time. Data existed once every 24 hours (at 00:00 UTC). While a higher resolution could be achieved by running MATCH over the Europe grid, lack of time for the project prevented doing this. Instead, the local run of MATCH for January was re-run with boundary values being fed in only once per day in order to estimate the impact of a lower resolution in the background concentration.

5 Gauss settings

The Gauss model was run for initial tests over February 2009, covering Stockholm city centre (see Figure 1), with a resolution of 100 × 100 m and with the EVA (s04) vehicle emission factors. A second run was made using the newer ARTEMIS (a07) emissions factors, the main difference between the two is an adjustment in the contribution from heavy and light vehicles (see Figure 2).
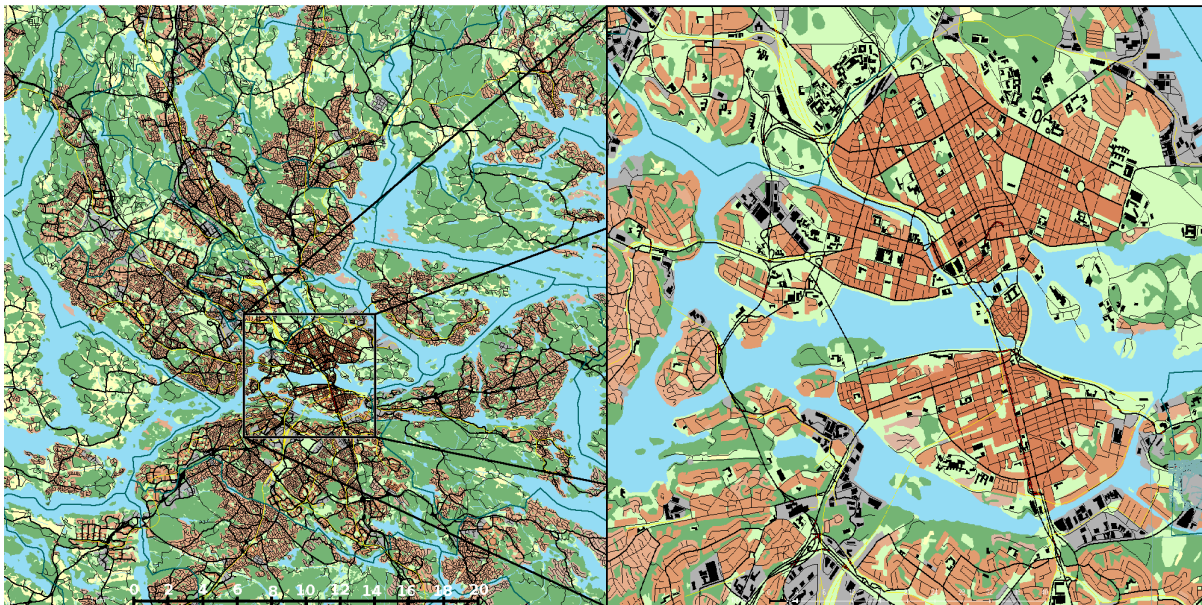
Figure 1: Gauss model coverage for metropolitan Stockholm (left) and Stockholm inner city (right).

The Gauss model was also run over February 2010 to be compared with the MATCH model. This run used the ARTEMIS emissions (a07), and covered the Stockholm metropolitan area (Figure 1) with a 500×500 m resolution.

6 Results

6.1 Comparison of the EVA and ARTEMIS Emissions

Annual Emissions (tons/year)		
	EVA	ARTEMIS
Light	356	303
Heavy	196	348
Total	552	651

Table 1: Annual emissions (tons/year) according to the EVA and ARTEMIS vehicle emission factors.

The weekly variation of emissions from EVA and ARTEMIS are presented in Fig-ure 2. These emissions represent mean values, and the true emissions vary more on a day-to-day basis. The total annual emissions are presented in Table 1 and shows that the total emissions in ARTEMIS are higher than in EVA.

The difference in model result due to emissions was tested by running the Gauss model for EVA and ARTEMIS separately. Figure 3 shows the NO_x content from the Gauss model calculations of two weeks in February 2009. The FB shows that the run using the EVA emissions under estimates the values while the ARTEMIS based run has a much smaller systematic bias. The higher NMSE together with the lower FB for ARTEMIS means that the random errors are larger than for EVA, since NMSE measures both systematic and random errors. This is mainly due to the higher peaks where the model over predicts the observed values. The high over prediction at 13-14 February, is also the main reason why the correlation is low for both runs. However, without the over prediction of
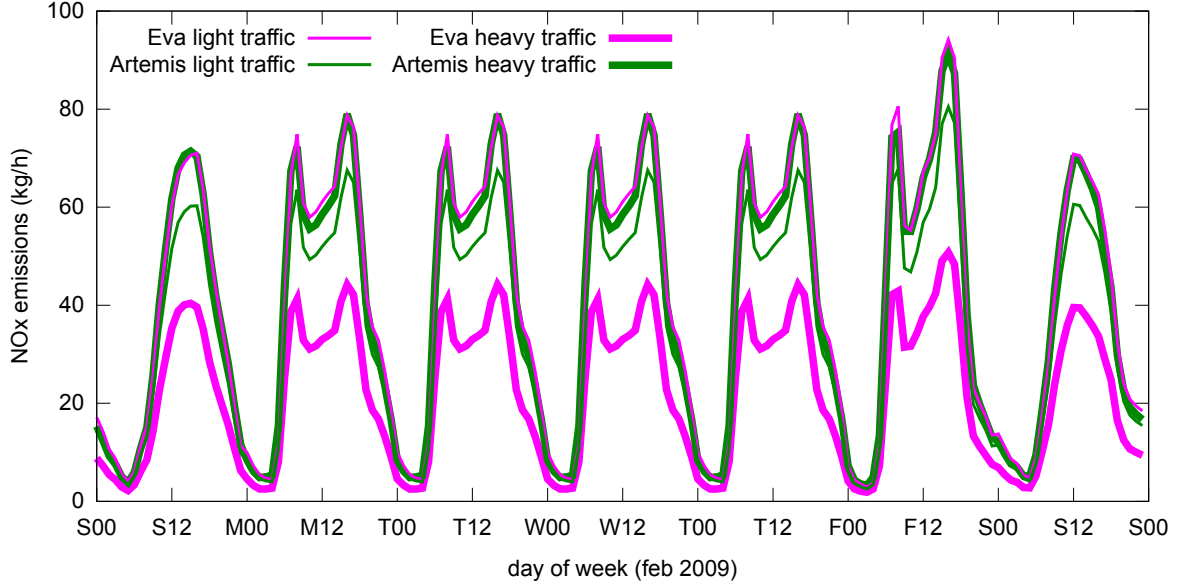
Figure 2: Weekly variation of emissions from road sources in Stockholm city centre for the EVA and ARTEMIS vehicle emission factors in kg/hour. The horizontal axis shows weekdays, *e.g.* M00 represents Monday 00:00 local time, W12 represents Wednesday 12:00. Mondays to Thursdays have the axact same emissions and fridays to sundays as well as odd holidays are treated differently. Heavy traffic (*e.g.* trucks, buses) and light traffic (*e.g.* cars, motorcycles) are treated separately. The main difference between ARTEMIS and EVA is a higher emission from heavy traffic in ARTEMIS

this period, the systematic errors would be larger.

6.2 MATCH Jan 2010

The NO_x content from the MATCH runs of February is shown in Figure 4 and the statistics are shown in Table 3. The first two runs (dd01 and dd15), which only differ from each other by the plume rise, give very similar result. The third run (ee01), which is the same as dd15 but is driven by meteorology with a higher resolution, gives slightly larger errors. This indicates that adjustments to the chimney emission heights have less impact on the final result than changes in meteorology. Which in turn suggests that the main NO_x emissions are not from chimneys. The FB and MG show small systematic errors for all runs, which compared with the NMSE and VG mean that the total error between model

Instance	med	25%	75%	FAC2	FB	MG	NMSE	R	VG
EVA	10.2	5.0	20.2	0.49	0.20	1.29	3.02	0.33	2.64
ARTEMIS	11.8	6.0	23.9	0.56	0.00	1.09	3.11	0.30	2.57
Observations	14.5	7.1	27.4						

Table 2: Medians and 25-, 75-percentiles for Gaussian model runs comparing the EVA and ARTEMIS emissions, as well as statistics as described in Section 2.5. The statistics represent the same time series as are shown in Figure 3). Optimal values of the statistical measures are FAC2, MG, R, VG = 1 and FB, NMSE = 0.
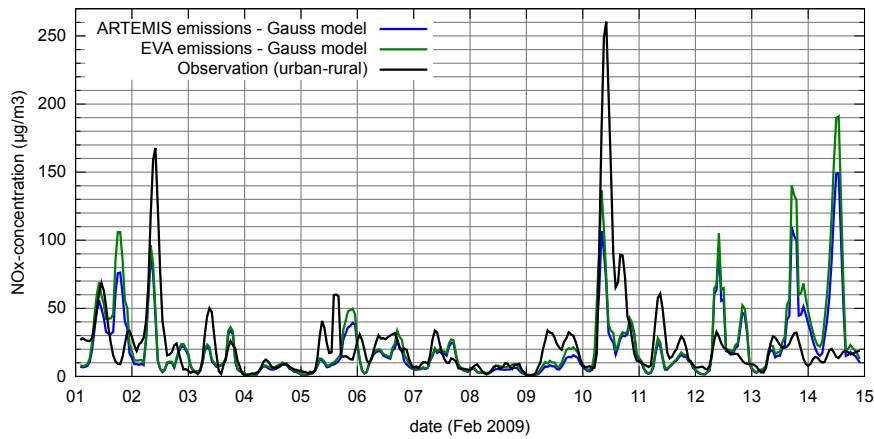
Figure 3: Three hour floating mean of NO_x concentrations ($\mu g/m^3$) for two weeks in February 2009. Two runs of the Gaussian model using different emission factors (EVA and ARTEMIS) ar presented as well as the observed concentrations. The observations are from TK with rural backgound concentrations (from NM) subtracted.
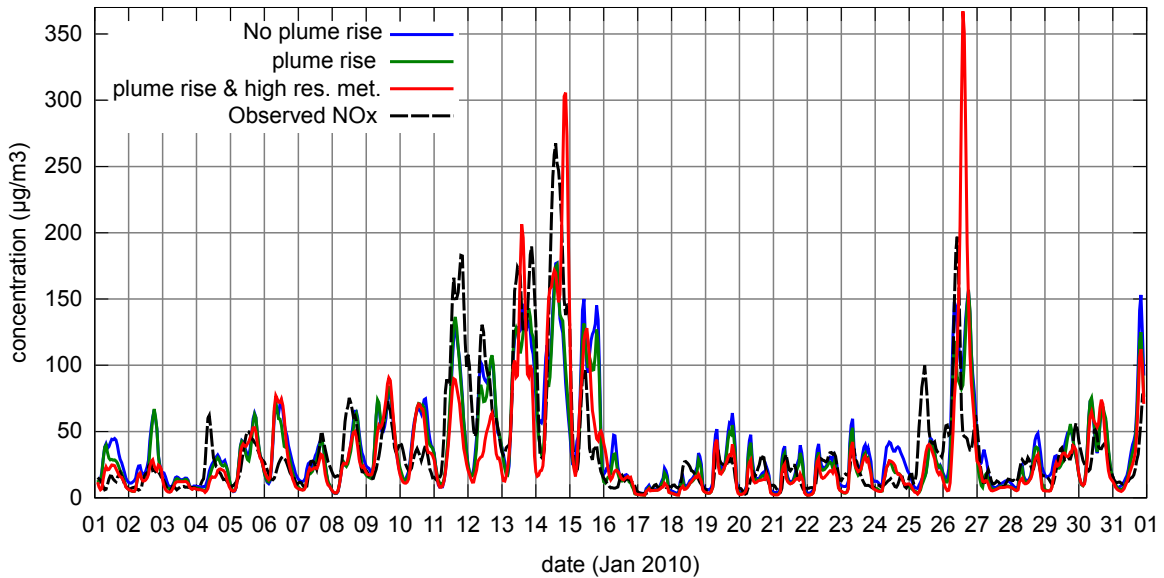

Figure 4: MATCH calculations and observations of NO_x at TK in 3h floating mean, Jan 2010. Three runs are presented; dd01 only emits in layer 1 (0-60 m), dd15 and ee01 has a 50% plume rise, yielding emissions in either layer 1, layer 2 (60-120 m) or layer 3 (120-210 m). dd01 and dd15 is driven by meteorology on a 22 km grid, ee01 uses an 11 km grid instead. The dispersion model (MATCH) is in all cases run with a resolution of 2 km.
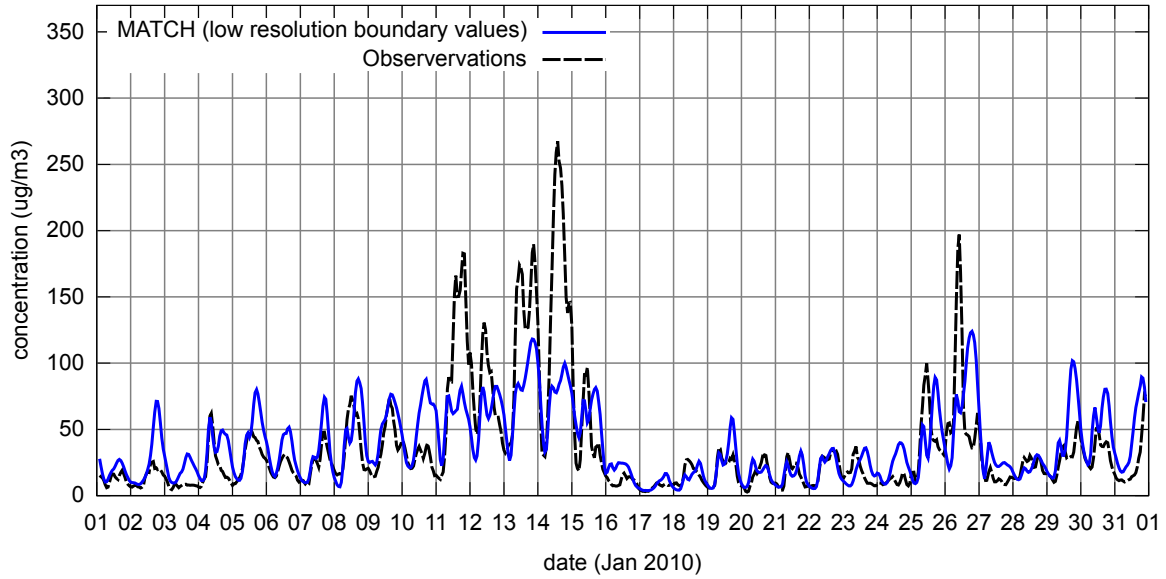
Figure 5: MATCH calculations and observations of NO_x at TK in 3h floating mean, Jan 2010. The MATCH run presented here reads boundary values (data at the edge of the model domain) once every 24 hours and uses the ARTEMIS emissions.

Instance	med	25%	75%	FAC2	FB	MG	NMSE	R	VG
No plume rise	25	13	50	0.69	-0.05	0.90	0.71	0.71	1.69
plume rise	21	9.6	43	0.69	0.06	1.10	0.70	0.74	1.71
plume rise & high res. met.	18	8.3	35	0.65	0.10	1.24	1.29	0.62	1.81
low res. boundary values	28	16	57	0.71	-0.05	0.79	0.79	0.65	1.48
Observations	21	11	39						

Table 3: Medians and 25-, 75-percentiles for the MATCH runs of January 2010, as well as statistics as described by Eq: (4)-(9). The three top rows represent the same time series as shown in Figure 4 and reads new boundary values every six hours. *"low res. boundary values"* read boundary values once per 24 hours. Optimal values are FAC2, MG, R, VG = 1 and FB, NMSE = 0.

and observation is dominated by unsystematic errors. Figure 4 also shows a clear build-up trend, at 10-15 January, which MATCH manages to reproduce.

Figure 5 shows the final MATCH run of January, using the same model settings and emissions as the February run (*i.e.* new boundary values at the edge of the model domain are read only once per 24 hours and the ARTEMIS (a07) emissions are used. The rightmost column (*low*) of Table 3 shows the statistics for this run. The errors are of the same magnitude as the other runs for January. This shows that the lower temporal resolution of the boundary values has little effect on the final result. However, it underestimates the high peaks between the 11th and 15th of February, which could be due to a stronger variation in boundary values during these days compared to the rest of the month.

6.3   Comparision of MATCH and the Gaussian model

6.3.1   Wind profiles

The results so far have shown that emissions are not the most important factor but rather the meteorology driving the dispersion, this is further investigated here by looking at wind fields. Figure 6 shows scatter plots of wind speed and direction, comparing observations with the calculated profiles used in each model for February 2010. The wind speeds used in the Gauss model are generally lower than the observations. The reason for this could be the "bluff body" effect, which is not treated by the wind model. A bluff body can be considered as the opposite of a streamlined body, where the flow is subject to a high Reynolds number, *e.g.* the flow around a building with sharp edges. At low Reynolds numbers the drag force on an object is dominated by the wind

shear. This is not the case for bluff bodies, where the main contribution to the drag force is due to the separation of boundary layer and inviscid region flow, Tritton (1988). The drag force can be interpreted as the pressure difference between the windward and leeward sides of a body. Thus an increase in the drag force, due to the bluff body effect, implies an increased pressure gradient past the body, which in turn forces a speed up in the nearby flow. Since the Reynolds number is proportional to wind speed, the speed up effect becomes more important at higher wind speeds, hence the increase in wind speed bias by increase in observed wind speed.

The wind speed from MATCH has a smaller systematic bias, but this value represents the mean wind speed of a 2×2 km wide and 60 m high grid box. Therefore, higher wind speeds should be expected due to the logarithmic wind profile.

The wind direction is very precise in the Danard model, since the model interpolates to the point where the observations are made, this is a very good result. The wind direction in MATCH differs more from the observations, but this is to be expected since it represents the mean wind direction of the entire grid box, and wind directions can vary alot in the surface layer, especially over a 2×2 km wide area.

Figure 7 shows the NO_x content by different wind directions for observations and model calculations. Gauss model and observations give the highest content for west-southwesterly winds and are overall similar. MATCH differs from the others, it gives the highest NO_x content at north-northwesterly winds. In general, MATCH gives higher concentrations around westerly winds than easterly.

MATCH differs from the other two charts for two reasons; first, the wind directions in MATCH differ more from observations than the wind fields used in the
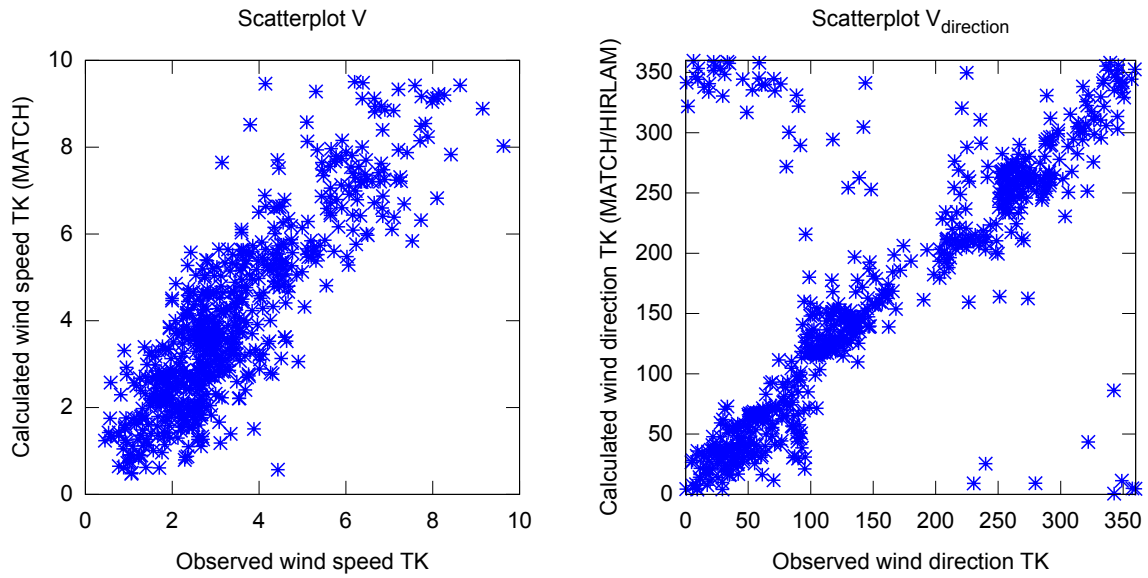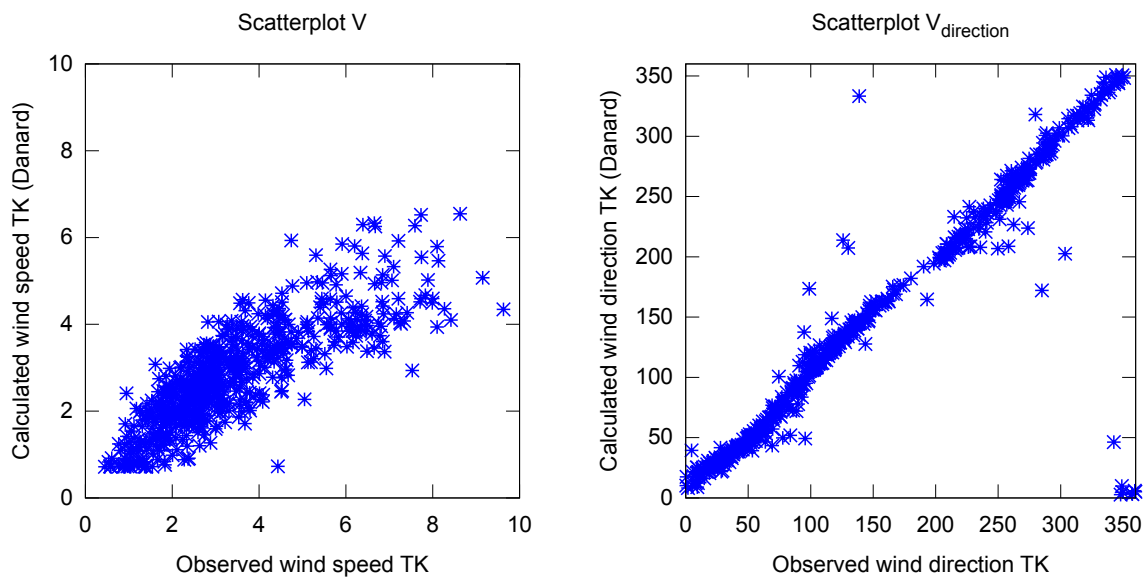
Figure 6: *Above:* Scatterplot of wind speed (left) and direction (right) between observations at TK and the calculated wind in the MATCH grid cell covering TK. *Below:* Scatterplot of wind speed (left) and direction (right) at TK between observations and the calculated wind profile used in the Gauss model
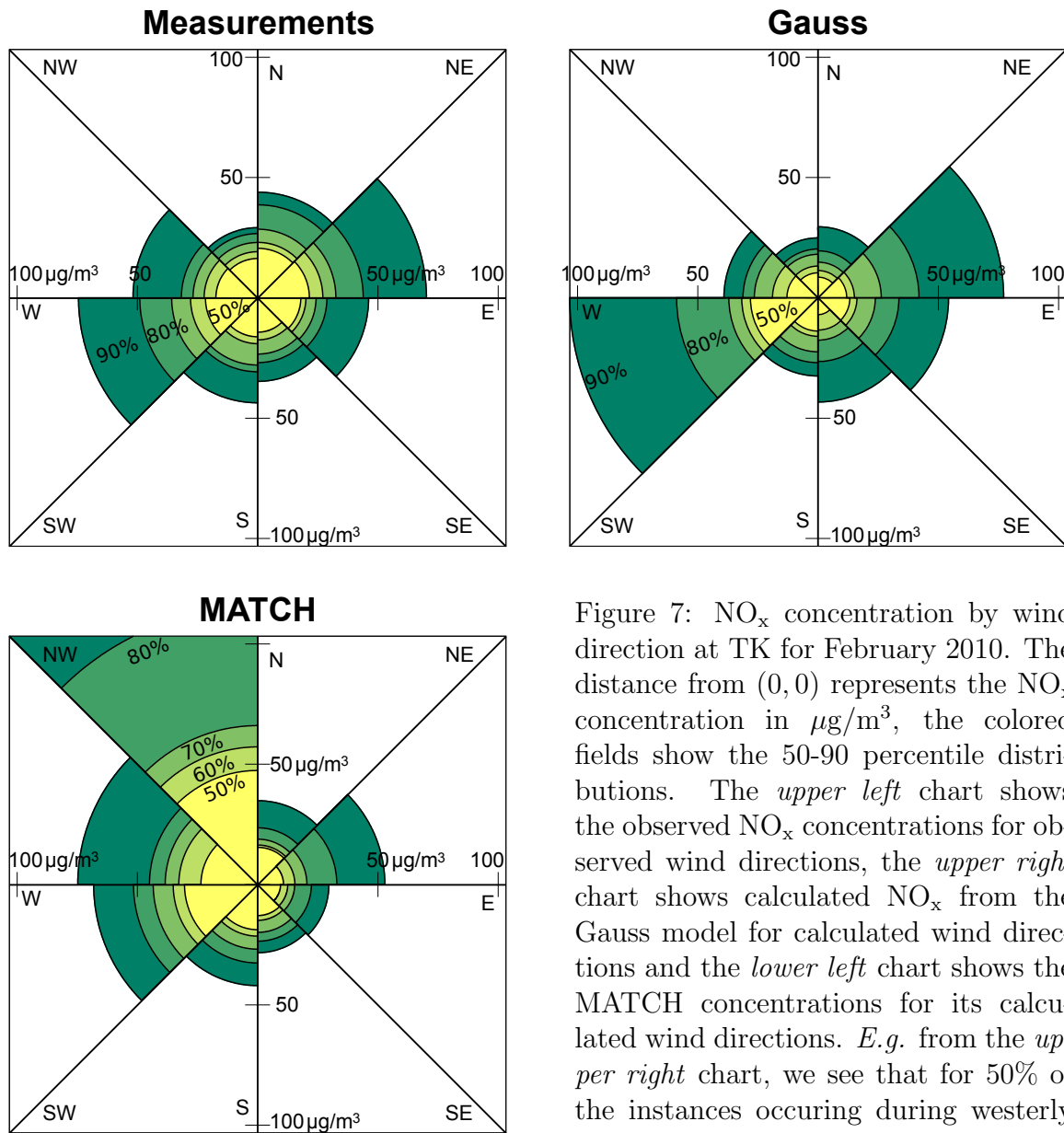
Measurements

Gauss

MATCH

Figure 7: NO_x concentration by wind direction at TK for February 2010. The distance from $(0,0)$ represents the NO_x concentration in $\mu g/m^3$, the colored fields show the 50-90 percentile distributions. The *upper left* chart shows the observed NO_x concentrations for observed wind directions, the *upper right* chart shows calculated NO_x from the Gauss model for calculated wind directions and the *lower left* chart shows the MATCH concentrations for its calculated wind directions. *E.g.* from the *upper right* chart, we see that for 50% of the instances occuring during westerly to south-westerly winds, concentrations are below $\sim 25\mu g/m^3$.

Gauss model. Second, the lower resolution in MATCH (2×2 km), compared to that of the Gauss model (500×500 m), affects the orientation of large emission sources, *e.g.* a large source located in a grid box adjacent to that which contains the observation site, might be included by the same grid box as the observation site at a lower resolution.

6.3.2 Comparision of NO$_x$ results

Comparison of NO$_x$ content by the models and observations is shown in Figure 8 and the corresponding statistics are presented in Table 4. MATCH values do not correspond to observations as well as for January. At first, this was believed to be due to the lower resolution in boundary values available for this period but the result from the final run in January (presented in Section 6.2) suggests otherwise.

The Gauss model has a larger FB than the MATCH run and a slightly larger MG *i.e.* the overall systematic error is larger for the Gauss model. Concerning random errors, the NMSE is of the same order for both MATCH and Gauss models but since the Gauss model has a larger systematic error, the NMSE implies that it has smaller random errors than MATCH. The higher correlation, R, for the Gauss model strengthens this arguement.

Comparing rural and urban performance of MATCH shows a lower correlation for the rural (NM) values, however, the FAC2 and FB are not significantly different and the NMSE is lower for the rural site. Thus by linear measures MATCH has better performance for rural values than urban. The MG shows a smaller systematic bias for the rural values. Finally, the VG shows a higher random error by logarithmic measures for the rural values. Overall, it seems that MATCH performs better for the rural content.

The accurate prediction of the peak in NO$_x$ at February 16th by the Gauss model is surprising. The wind speeds for this period were very low (0-0.5 m/s), as is shown in Figure 9, and the governing equation in the Gauss model is undefined for low wind speeds. Therefore it is to be expected that the model will be unrelialbe under such conditions, yet its result coincides very well with observations. The low wind speeds throughout the day is one of the reasons for the extreme peak, but similar wind speeds are seen at February 9th as well and the corresponding NO$_x$ content does not stand out from the rest of the data set. The reason why the peak on the 16th stands out more is due to a difference in stability. Temperature differences from observations at different heights can be used as a measure of the lower boundary layer stability. Such temperature observations from Högdalen show neutral conditions on the 9th of February but stable conditions in the morning on the 16th. The reason for the peak on the 16th of February could therefore be the result of the combination of high stability and low wind speeds during rush hour. However, the observations lack regional background data for this period so it is possible that the observed peak is not as high as it seems. This also excluded the values from the statistics, which is probably for the better since the linear measures (*i.e.* FB, NMSE, R) would be strongly influenced by it.

The weekly variation of NO$_x$ concentrations in February 2010 is shown in Figure 10. Due to the presence of extreme outliers in the data set, the median is presented instead of the mean. The Gauss model follows observations better than MATCH for most days and clearly has a smaller systematic bias. The MATCH model seems to follow the same shape as the observed values Modays to Fridays
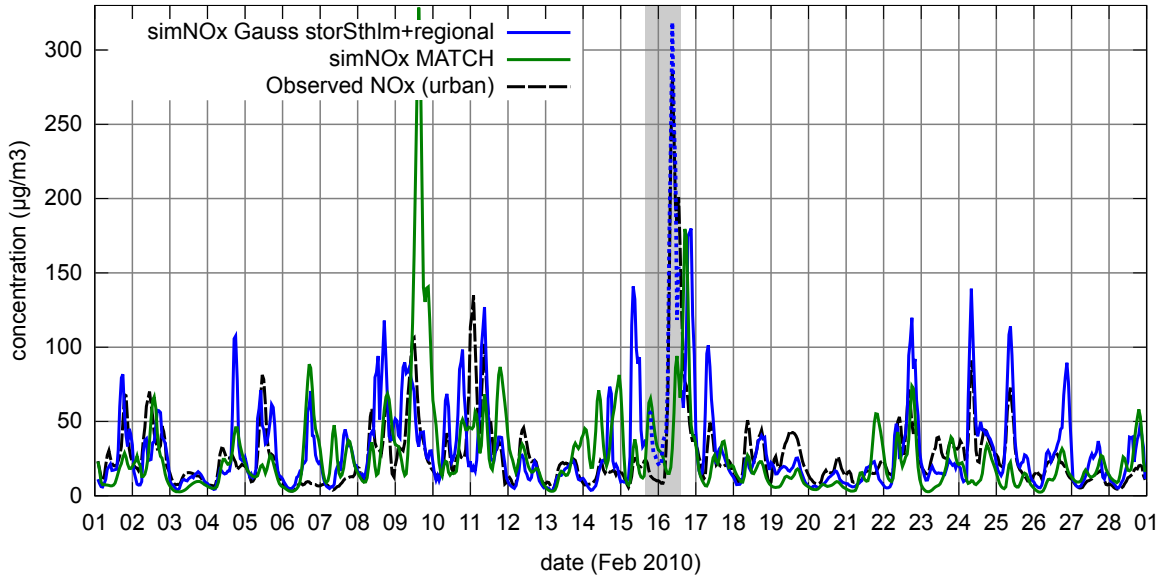
Figure 8: 3h floating mean of NO_x content in February 2010, the three time series show: Calculated content at TK by the Gauss model with observed regional background content (from NM) added, MATCH calculations and observations at TK. The shaded area represents the Gauss results where observations at NM are missing.

Instance	med	25%	75%	FAC2	FB	MG	NMSE	R	VG
Gauss	13.4	5.8	28.6	0.47	-0.34	0.88	1.98	0.36	2.59
MATCH (TK)	16.9	9.4	32.6	0.55	0.01	1.12	1.97	0.30	2.31
MATCH (NM)	5.0	3.1	8.3	0.55	0.03	0.99	1.85	0.07	2.66
Observations (TK)	19.2	11.5	30.7						
Observations (NM)	4.5	3.2	8.5						

Table 4: Comparision of NO_x concentrations for the model runs of February 2010, the first set of columns show the medians and 25- and 75-percintiles. The next set shows statistical measures as described in Section 2.5. Gauss compares the Gauss model run with urban observations (with the regional background content subtracted), MATCH TK and NM compares MATCH runs and observations at the urban site (TK) and the rural site (NM). The last two rows show the median and percentile values for observations at TK and NM.
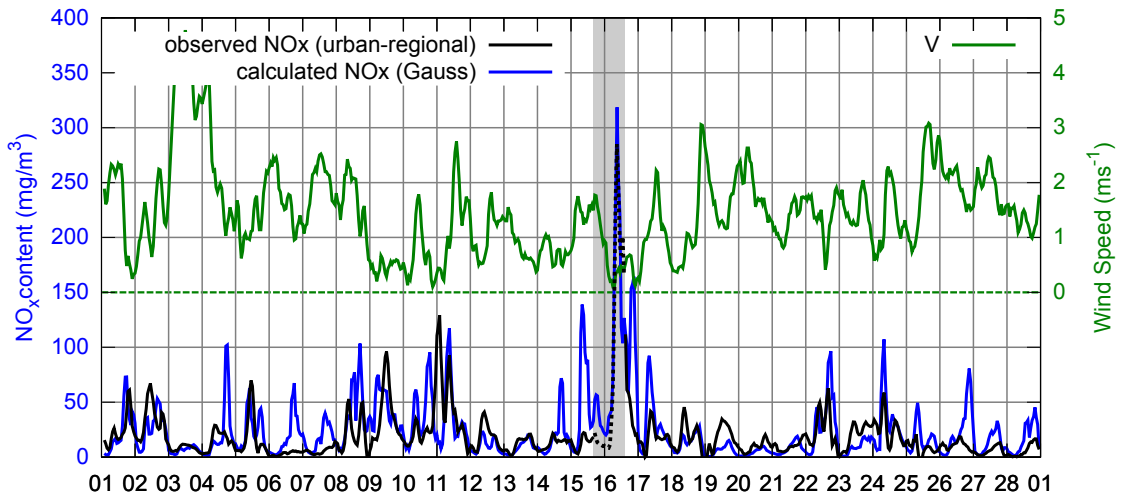
Figure 9: 3h floating mean of NO_x content together with observed wind speeds in February 2010. The left axis shows NO_x concentrations in $\mu g/m^3$ the corresponding time series are urban observations, TK, (with rural content, NM, subtracted) and Gauss model results. The shaded area represents a preiod where rural measurements from NM are missing. The right axis shows wind speeds for observations at Högdalen.
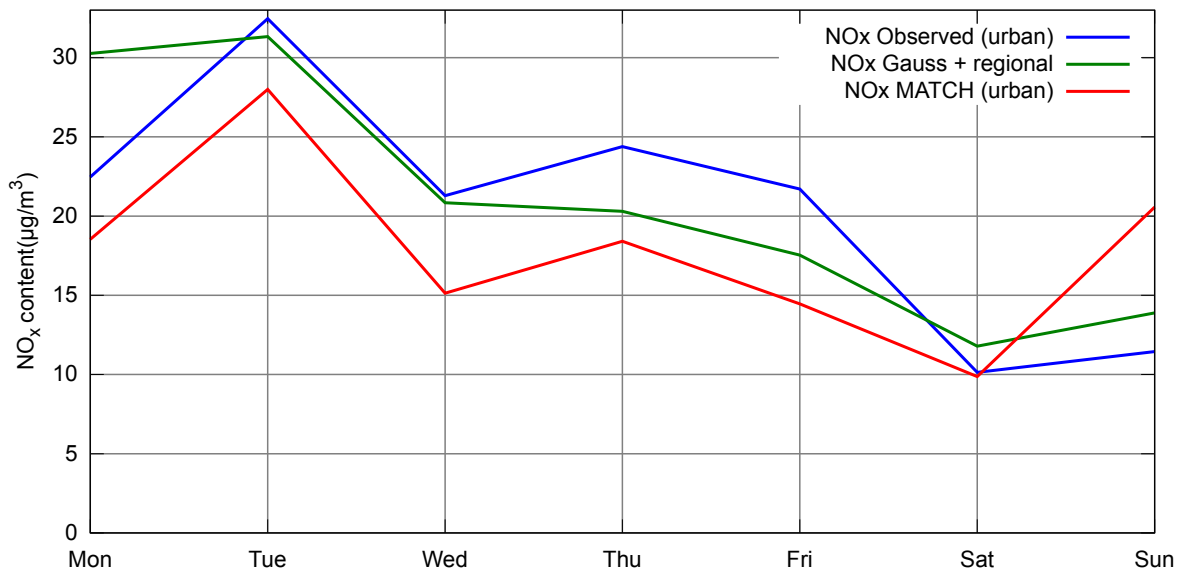

Figure 10: Median weekly variation of NO_x concentration in $\mu g/m^3$ for February 2010. "Observed (urban)" shows the observations at TK, "Gauss+regional" shows the Gauss calculations with rural content added (from observations at NM) and "MATCH (urban)" shows the MATCH results.

but with a systematic bias. Both models are within 30% of the observed values for most weekdays, with the exception being MATCH on Sundays. This suggests that the models are able to describe the day-to-day variation with acceptable precision.

Figure 11 shows the hourly median of NO_x content during February. The Gauss model follows observations from about 00:00 to 15:00 very well. MATCH does not coincide as well with observations, but there is a qualitative similarity from morning to midday. Both models predict a strong peak in the afternoon which is not seen in the observations. There is probably a significant error in a parameter used by both models. This could be due to emissions, since these follow the same diurnal variation for weekdays, with a maximum in emissions in the afternoon. However, this peak is not much higher than the emissions in the morning, therefore, the Gauss model should not give a much higher peak in the afternoon solely due to the slight increase in emissions. Especially since the boundary layer is generally less stable in the afternoon, which means that the pollutants will not be trapped in a near surface inversion. The fact that both models estimate the same peak suggests that the problem does not lie within the models and it is probably not meteorology either since the models use different methods to estimate meteorological data, which would mean that an error occuring in the input of one model should not appear in the other. In addition, Figure 11 shows the median for the entire month, unless the "errors" behind the peak appear regularly, they would not show up at all.

6.4 Gaussian model and PM_{10}

Figure 12 shows the PM_{10} content for February 2010, there were no boundary values available for the MATCH run, thus only the Gauss result is presented. The PM_{10} content during this period is completely dominated by the long distance transport which is seen by comparing the two observation sites; both sites give concentrations of the same magnitude and the rural content is often higher than the urban.

This can be explained by street wetness, as is shown by Norman and Johansson (2006). Under dry conditions road dust is easily suspended by the wear of tires. A wet surface will bind the dust particles and prevent suspension. The street wetness in Stockholm for this period (as well as February 2009) is shown in Figure 13, it shows a high street wetness throughout February 2010. This results in the local sources of PM being very low. The Gauss model does not take this into account but uses the same emissions regardless of street wetness, as is also seen in Figure 12.

The low local contribution to PM_{10} over February can also be shown by looking at air parcel trajectories for the period, Figure 14 shows backward calculated trajectories from Stockholm ($59.33°$ N $18.08°$ E), 11:00 UTC each day. The calculations are from the NOAA (National Oceanic and Atmospheric Administration) HYSPLIT (HYbrid Single Particle Lagrangian Integrated Trajectory) model. Calculations are made automatically each day and stored at SLB. Calculated trajectories are more reliable the straighter and smoother they are. Sharp turns indicate strong wind velocity gradients (spacial or temporal) or very low wind speeds, calculating reliable trajectories is difficult in both cases.

The trajectory for the 6th of February passed over parts of eastern Europe 18-48 hours before reaching Stockholm. This region is a large source of PM from coal combustion and the PM_{10} content this day
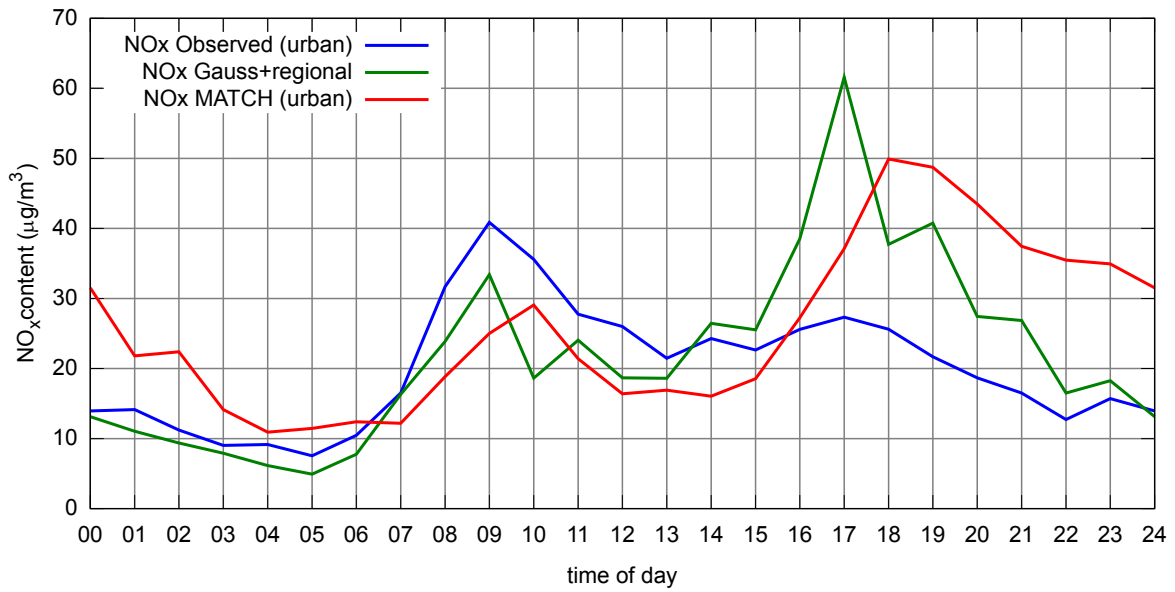
Figure 11: The median diurnal variation of NO_x concentrations ($\mu g/m^3$) during February 2010, "Observed (urban)" shows observations at TK, "Gauss+regional" shows the Gauss result with rural content (observations from NM) added, "MATCH (urban)" shows the MATCH results.
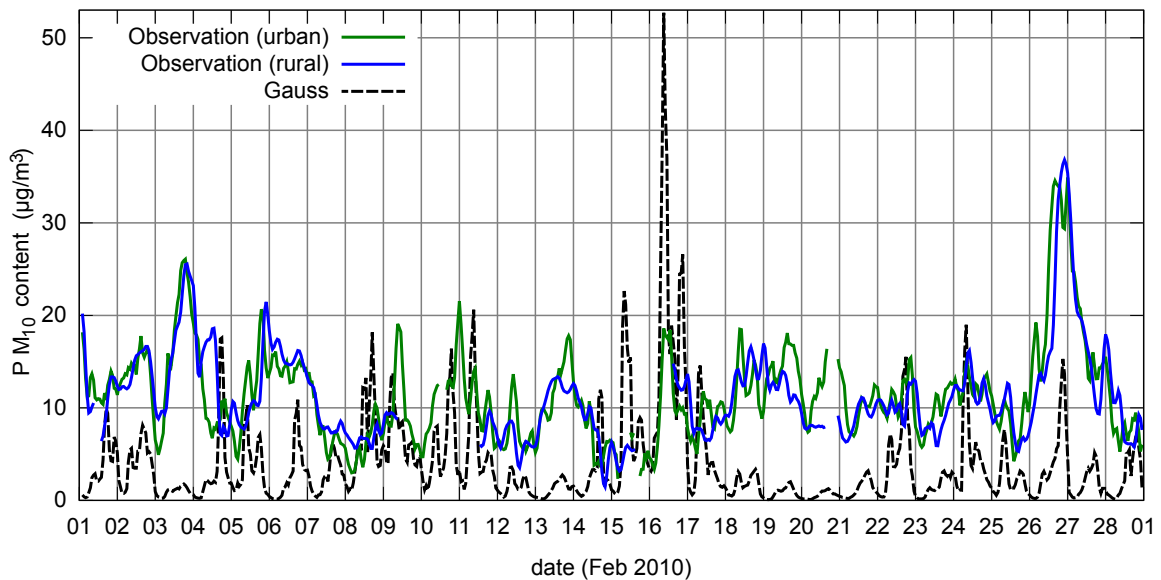

Figure 12: 3 h floating mean of PM_{10} concentrations ($\mu g/m^3$) for urban and rural observations, as well as Gauss model calculations of February 2010.
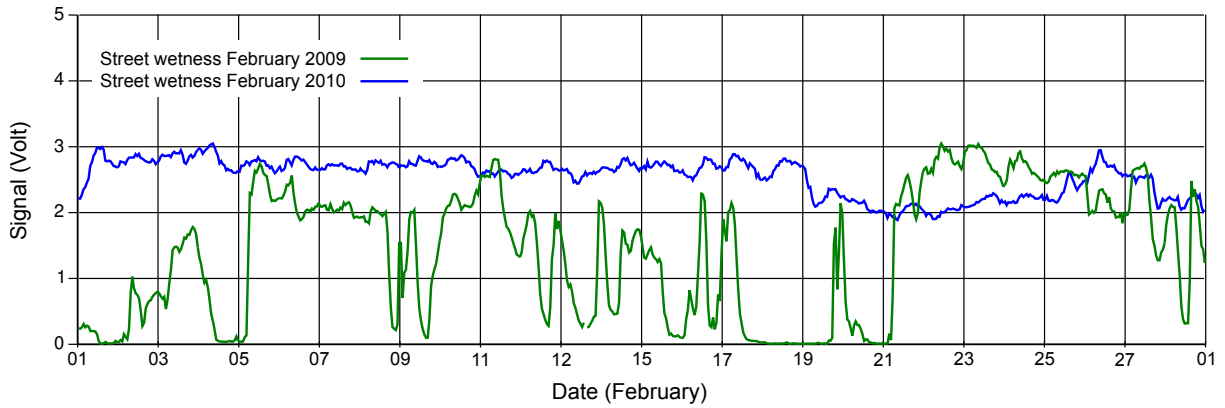
16

Figure 13: Observed street wetness for February 2009 and 2010. Observations are made at three streets in the city centre; Hornsgatan, Norrlandsgatan and Sveavägen. Each site measures the wetness by resistance wires at three points in the street. The figure shows the mean voltage signal from all observations, a high voltage means the road is wet, zero represents a dry surface. (The 2009 wetness is included for comparision)

was above 12 μg/m^3. During the following days, 7th-8th, the trajectories trace back over the Nordic seas, which should result in very clean air. The PM$_{10}$ content during these days was indeed lower, (Figure 12). The trajectory of the 9th is not as reliable since it is near stationary during its last 24 hours. This may be the reason for the peak in PM$_{10}$ near midday but it is also likely that this due to transport from elsewhere since both the rural and urban stations register the same peak. During the 10th, the trajectory once again passes over eastern Europe and the PM$_{10}$ content increases to 12 μg/m^{3}at the arrival of the air parcel. The same reasoning can be applied to most of the months but there are some interesting exceptions.

The peak in PM$_{10}$ on the 16th of February is probably not due to any long distance transport. The trajectory is near stationary for more than 24 hours and measurements made show wind speeds of 0-0.5 m/s for the entire day. This is the same peak as was seen for the NO$_x$ calculations (and observations) in Section 6.3.2. It can be explained in the same way, *i.e.* stable conditions and low wind speeds dur-

ing rush hour, but PM$_{10}$ observations show a lower peak. The model sees the same conditions as for NO$_x$ but the observations give a lower values since the emissions are lower due to road wetness.

An interesting point here is the similarity of the NO$_x$ and PM$_{10}$ results. In fact, the main difference between the NO$_x$ and PM$_{10}$ emissions in the EDB is a scalar, the sources used are the same (mainly road emissions) and the Gauss model treats both trace species the same way. Figure 15 shows the NO$_x$ and PM$_{10}$ content at TK plotted on different y-axes to show the similarity. The two series follow each other almost perfectly.

7   Conclusions

The strong influence of meteorology as suggested in Section 6.2, is very important since both models use the same weekly variation in emissions all year around. These emissions are mean values and the true emissions vary more on a day-to-day basis. Therefore, it is a good thing that the model result is poorly affected by changes in emission sources. However, the different
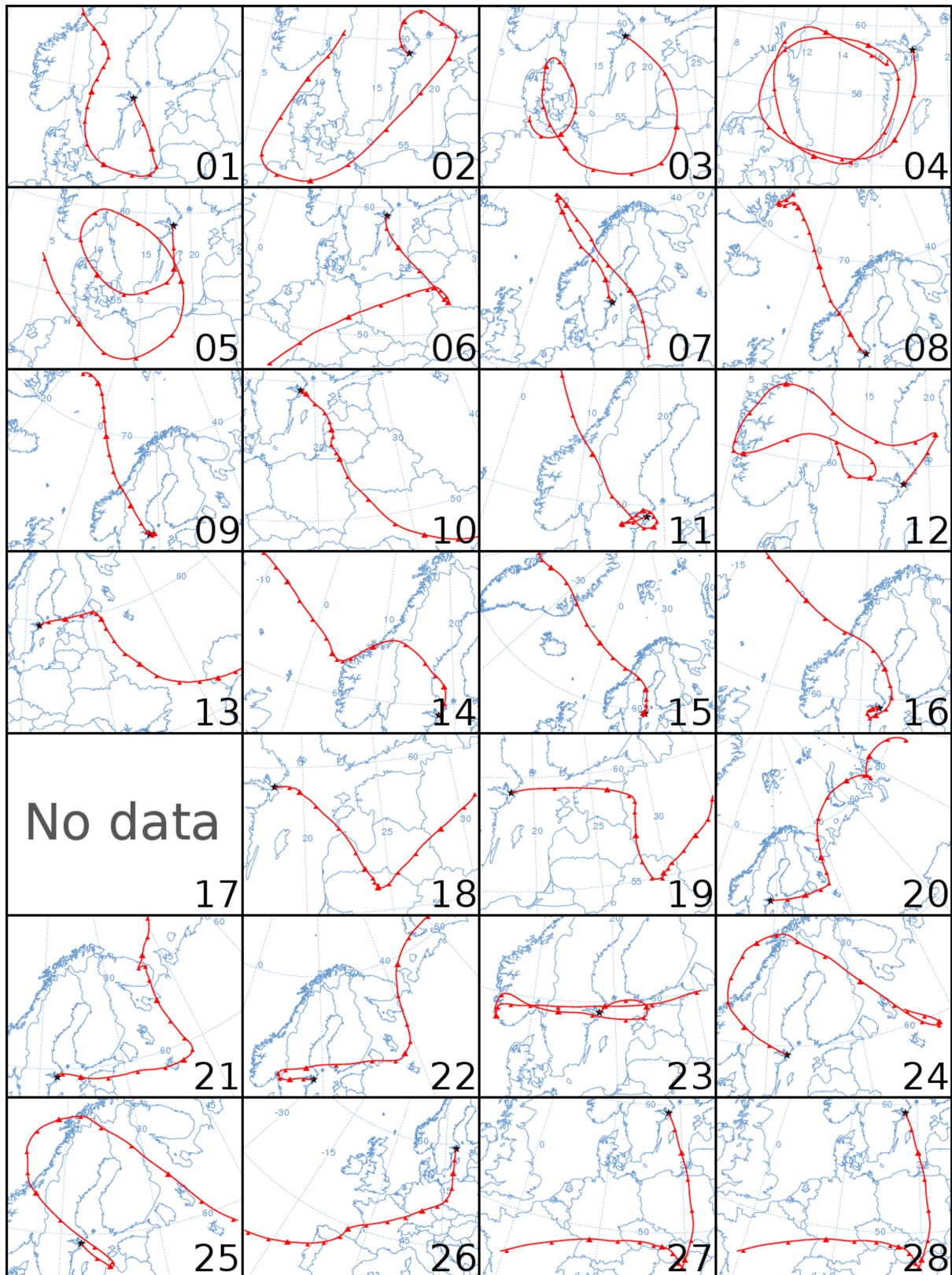
Figure 14: Backward calculated trajectories ending at 11:00 UTC each day in February 2010. The source from which the trajectories are calculated is 59.33° N 18.08° E (Stockholm). Calculations were made using the NOAA HYSPLIT model.
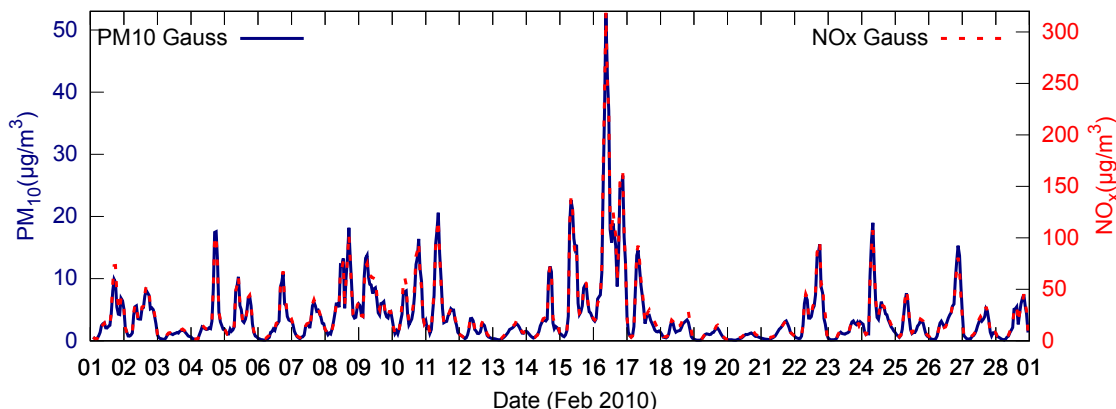
Figure 15: Comparision between NO_x and PM_{10} from Gauss model runs over February 2010.

emission factors compared only differ by a scalar for each road segment, the peaks and dips in emission rates occur at the same time for both.

MATCH turned out to be more reliable for regional conconentrations than urban. This is credible due to its lower resolution (2×2 km) as opposed to the Gauss model (500×500 m), which may be too rough to fully represent the complicated emissions and dynamics in cities. Errors from observations should also be taken into account. The observations at TK are used as the urban background values which assumes that the site is not affected by any direct emission. This is a simplification and an unachievable ideal.

The comparision of temporal resolution in boundary values for the MATCH model, showed that the higher resolution (new data every 6 hours as opposed by 24 hours for the lower resolution) is not always necessary to give a satisfactory result. However, some periods have a stronger variation in the boundary values, and it is thus advisable that the higher resolution is used.

The fact that NO_x and PM_{10} is more or less treated the same way by the Gauss model makes an interesting point. It could

be useful to include an algorithm for adjusting the emissions depending on street wetness. As was shown for February 2010, the Gauss model constantly over estimated the local contribution to PM_{10} concentrations since street wetness was not included in the model.

The wind directions from the Danard wind model turned out to be very precise, which is of importance to the Gauss model, since it directly affects the trajectories of the plumes.

7.1 Outlook

The difference in performance for the January and the February run of MATCH was not fully explained. As was suggested in Section 4, it would be interesting to run the model again with better boundary value resolution for February. There could be a stronger diurnal variation in the boundary values in February than in January, which might explain the difference in performance.

Precision of the wind model might be improved if the Bluff Body effect was to be treated by the wind model, but doing this on such a large scale as an entire city would require immense comput-

ing power; Tseng et al. (2006) shows that in order to accurately simulate the Bluff Body flow in an urban environment, using Large Eddy Simulation, a horizontal resolution of less than 5×5 m is required. It is therefore clear that adjustments should be made elsewhere if overall improvement of the Gauss model is desired.

References

Bott, A., 1999: A positive definite advection scheme obtained by non-linear renormalization of advective fluxes. *Monthly Weather Review*, **117**, pp. 1006-1015.

Chang, J. C. and S. R. Hanna, 2004: Air quality model performance evaluation. *Meteorology and Atmospheric Physics*, **87**, pp. 167-196.

Tseng, Yu-Heng, Charles Meneveau and Marc B. Parlange, 2006: Modeling Flow around Bluff Bodies and Predicting Urban Dispersion Using Large Eddy Simulation *Environmental Science & Technology*, **40**, pp. 2653-2662.

Danard, M., 1976: A Simple Model for Mesoscale Effects of Topography on Surface Winds. *Monthly Weather Review*, **105**, pp. 572-581.

Holtslag,. A. A. M., 1984: Estimates of diabatic wind speed profiles near-surface weather observations. *Boundry-Layer Meteorology*, **29**, pp. 225-250.

Norman, Michael, Christer Johansson, 2006: Studies of some measures to reduce road dust emissions from paved roads in Scandinavia. *Atmospheric Environment*, **40**, pp. 6154-6164

Robertson, Lennart, Joakim Lagner, Magnuz Engardt, 1999: An Eulerian Limited-Area Atmospheric Transport Model. *Journal of Applied Meteorology*, **38**, pp. 190-210.

Tritton, D. J., 1988: *Physical fluid dynamics, 2nd revised edition.* Oxford, Clarendon Press, ???, 536 pp.

Wallace, John M., Peter V. Hobbs, 2006: *Atmospheric Science, an introductory survey.* Elsevier Academic Press, San Diego, California, USA, 488 pp.

Zannetti, Paolo, 1990: *Air pollution modelling: Theories, Computational Methods and Available Software.* Computational Mechanics Publications, Southhampton, UK, 444 pp.

A Terminology

EDB	Emission Data Base
HYSPLIT	HYbrid Single Particle Langragian Integrated Trajectory model
NM	rural observation site Norr Malma, outside Norrtälje
NO_x	Nitrogen oxides (NO and NO_2)
MATCH	Multiple Scale Amtospheric Transport model
NOAA	National Oceanic and Atmospheric Administration
PM_{10}	Particulate Matter with a typical diameter of less than $10\mu m$
SMHI	Swedish Institue for Meteorology and Hydrology
TK	urban observation site at Torkel Knutsson gatan, Södermalm, Stockholm
weekday	ordinary weekdays (mon-thu) not holidays

Acknowledgements